Received: 17 September 2020 | Revised: 23 December 2020 | Accepted: 7 January 2021

DOI: 10.1096/fj.202001767R

RESEARCH ARTICLE

THE FASEB JOURNAL

New GFAP splice isoform (GFAPμ) differentially expressed in glioma translates into 21 kDa N-terminal GFAP protein

Emma J. van Bodegraven[1] | **Jacqueline A. Sluijs**[1] | **A. Katherine Tan**[1,2] | **Pierre A. J. T. Robe**[2] | **Elly M. Hol**[1]

[1]Department of Translational Neurosciences, University Medical Center Utrecht Brain Center, Utrecht University, Utrecht, The Netherlands

[2]Department of Neurology and Neurosurgery, University Medical Center Utrecht Brain Center, Utrecht University, Utrecht, The Netherlands

Correspondence
Emma J. van Bodegraven and Elly M. Hol, Translational Neuroscience, Brain Center Rudolf Magnus, University Medical Center Utrecht, Universiteitsweg 100, 3584 CG Utrecht, The Netherlands.
Email: e.m.hol-2@umcutrecht.nl

Funding information
Nederlandse Organisatie voor Wetenschappelijk Onderzoek (NWO), Grant/Award Number: 865.09.003; KWF Kankerbestrijding (Dutch Cancer Society), Grant/Award Number: KWF 10123; T&P Bohnenn fund

Abstract

The glial fibrillary acidic protein (GFAP) is a type III intermediate filament (IF) protein that is highly expressed in astrocytes, neural stem cells, and in gliomas. Gliomas are a heterogeneous group of primary brain tumors that arise from glia cells or neural stem cells and rely on accurate diagnosis for prognosis and treatment strategies. GFAP is differentially expressed between glioma subtypes and, therefore, often used as a diagnostic marker. However, GFAP is highly regulated by the process of alternative splicing; many different isoforms have been identified. Differential expression of GFAP isoforms between glioma subtypes suggests that GFAP isoform-specific analyses could benefit diagnostics. In this study we report on the differential expression of a new GFAP isoform between glioma subtypes, GFAPμ. A short GFAP transcript resulting from GFAP exon 2 skipping was detected by RNA sequencing of human glioma. We show that GFAPμ mRNA is expressed in healthy brain tissue, glioma cell lines, and primary glioma cells and that it translates into a ~21 kDa GFAP protein. 21 kDa GFAP protein was detected in the IF protein fraction isolated from human spinal cord as well. We further show that induced GFAPμ expression disrupts the GFAP IF network. The characterization of this new GFAP isoform adds on to the numerous previously identified GFAP splice isoforms. It emphasizes the importance of studying the contribution of IF splice variants to specialized functions of the IF network and to glioma research.

KEYWORDS

GFAP, glioma, alternative splicing, GFAP isoforms, intermediate filaments

1 | INTRODUCTION

Glial fibrillary acidic protein (GFAP) is a type III intermediate filament (IF) protein, which forms together with vimentin, synemin, and nestin the cytoskeletal IF-network in astrocytes. GFAP is often used as a marker of astrocytes, and increased expression of GFAP as an indicator of reactive gliosis in the injured and diseased brain.[1,2] Moreover, GFAP is a classical diagnostic marker for the most malignant tumors of the central nervous system (CNS); gliomas.[3-5] Gliomas are

Abbreviations: 1p/19q, short arm of chromosome 1/long arm of chromosome 19; CDS, coding sequence; CNS, central nervous system; FBS, fetal bovine serum; GFAP, glial fibrillary acidic protein; IDH1, isocitrate dehydrogenase 1; IF, intermediate filament; ihNSCs, Human immortalized fetal neural stem cells; PTC, premature termination codons; TCGA, the cancer genome atlas; UTR, untranslated region.

Pierre A. J. T. Robe and Elly M. Hol share senior authorship.

a large and diverse group of primary brain tumors that arise from glia cells or their precursors, and GFAP is differentially expressed between glioma subtypes.[6]

However, the GFAP gene is highly regulated by the process of alternative splicing.[7,8] Up to now, the expression of eight different human GFAP transcripts has been confirmed; the canonical variant GFAPα,[9] GFAPδ,[10,11] GFAPγ,[12] GFAPκ,[13] GFAPΔ135,[14] GFAPΔ164,[14] GFAPΔexon6,[14] and recently GFAPλ.[15] These GFAP isoforms are expressed in specific cell types of the CNS, such as radial glia and adult neural stem cells, in reactive gliosis in Alzheimer's disease and epilepsy, in Alexander's disease, and in glioma.[1,15,16] The isoforms are generated by the in- or exclusion of an intronic or exonic region that changes the coding sequence (CDS) of the transcript, the 5′ untranslated region (UTR), and/or the 3′ UTR.

In recent years, higher resolution methods such as RNA sequencing have shown that the level of RNA processing varies between tissue types, developmental stages, and between healthy and diseased tissues.[17-20] Altered RNA splicing[21,22] and increased 3′UTR shortening[23] are observed in various cancer types. For example, alternative splicing events that result in premature termination codons (PTC) are more often observed in cancer compared to healthy tissue.[24] Expression of transcripts that contain a PTC, but that are not degraded by the mechanism of nonsense-mediated RNA decay, results in the translation of shorter proteins.[25] As changes in RNA processing can function as a pro-oncogenic mechanism,[26] targeting RNA processing to treat cancer is currently under investigation.[22]

In our previous studies, we have reported on alterations in GFAP alternative splicing in glioma. We have observed that in high malignant glioma the relative level of the alternative splice variant GFAPδ to the canonical variant GFAPα is increased compared to lower malignant glioma[27] and in vitro studies suggest that changes in the relative level of GFAPδ to GFAPα have functional implications for glioma.[27-29] These studies emphasize the importance of discriminating between GFAP splice variants when studying the role of GFAP in glioma malignancy and using GFAP as a diagnostic marker.[6]

We here report on the differential expression of a new GFAP isoform in glioma of different grades of malignancy, GFAPμ. Based on the annotated sequence in the RNA sequencing data of human glioma (The Cancer Genome Atlas) we identified GFAPμ as a product of skipping of GFAP exon 2. This leads to the generation of a transcript with a PTC in exon 3 and consequently an extremely short CDS. We confirm the endogenous expression of GFAPμ mRNA in different types of tissue and cells and show translation of GFAPμ cDNA into a ~21 kDa sized GFAP protein that is detected in the human spinal cord as well. We further characterize GFAPμ upon its induced expression in different cell lines and describe how its expression influences the IF network.

2 | MATERIALS AND METHODS

2.1 | RNA sequencing TCGA data analysis

RNA sequencing data of 165 grade IV glioma and 306 low-grade glioma (including glioma of the astrocytoma histological subtype) were obtained from the cancer genome atlas (TCGA). Normalized RNA isoform expression data (Level 3 released data downloaded June 2015) were extracted as upper quantile normalized RSEM (RNA-Seq by Expectation Maximization) count estimates (normalized expression). Recurrent tumors were removed, and normalized counts of duplicate tumor samples were averaged. Isocitrate dehydrogenase 1 (IDH1) and short arm of chromosome 1/long arm of chromosome 19 (1p/19q) status information was available for 144 grade IV glioma and 282 low-grade glioma. For grade IV glioma, processed broad mutation data were downloaded from the UCSC Cancer Browser in June 2015. For low-grade glioma data were extracted from the TCGA network publication of 2015.[30] Gliomas were categorized according to the World Health Organization classification system of 2007 (histological subtypes) or 2016 (molecular subtypes). Table S1 contains information on the included patient cohort.

2.2 | Sample collection

Fresh frozen healthy temporal cortex tissue from three different donors was provided by the Netherlands Brain Bank (NBB; hersenbank.nl). Tissue was lysed using TRIzol reagent (Ambion by Thermo Scientific). Primary adult neural stem cells were isolated from postmortem brain tissue and lysed according to a previously described protocol.[31] Primary glioma cells were obtained from tumor tissue of patients undergoing resection surgery for glioma grade IV at the University Medical Center Utrecht. Tumor tissue samples were placed directly into tissue culture flasks and maintained in DMEM/F-12 (Gibco, Thermo Scientific) supplemented with 100 U/mL penicillin, 100 μg/mL streptomycin (1% p/s), and 10% (v/v) Fetal Bovine Serum (FBS) (all Invitrogen, Bleiswijk, The Netherlands). Cells were passaged at confluence for maintenance and collected and lysed using TRIzol reagent (Ambion by Thermo Scientific). IF fractions from human spinal cord were obtained as described previously.[32]

2.3 | Cell lines and culture

All cell lines were maintained at 37°C in a humidified incubator with 5% CO_2. U251-MG glioma cells (obtained from Muenster, Germany) were maintained in DMEM high glucose: Ham's F10 nutrient mix, supplemented with 1% p/s and 10% FBS (all Invitrogen). The identity

of U251-MG cells was confirmed by short terminal repeat analysis (Eurofin, Luxembourg). Human embryonic kidney 293 cells (293T) were maintained in DMEM high glucose supplemented with 1% p/s and 10% (v/v) FBS. The adrenal carcinoma cell lines SW13.Vim- and SW13.Vim + were maintained in DMEM:Ham's F12 nutrient mix and glutaMAX supplemented with 1% p/s and 5% (v/v) FBS. Human immortalized fetal neural stem cells (ihNSCs)[33] were maintained in Euromed-N medium (EuroClone, Amsterdam, The Netherlands), 1% N2 (5.375 mL DMEM-F12 (Gibco, Thermo Scientific), 0.75% BSA, 62.5 mg insulin (Sigma), 100 mg apo-transferrin (Sigma), 10 µL 3 mmol/L Na-Selenite (Sigma), 16 mg Putrescine (Sigma), 20 µg Progesterone (Sigma), 1% glutaMAX (Gibco), 1% L-glutamin (Gibco), 1% p/s, 20 ng/mL EGF, and 10 ng/mL FGF (both Tebu-Bio).

2.4 | RNA isolation

For RNA isolation of cell lines, cells were plated at a density of 4×10^4 cells per well in a 24-well plate. After 3 days cells were lysed using TRIzol (Ambion by Thermo Scientific). To extract RNA from lysed tissue and cell line samples in TRIzol, chloroform (EMD Millipore Inc, Darmstadt, Germany) was added and by centrifugation at 12 000 *g* at 7°C for 15 minutes, RNA was separated from proteins and lipids. RNA was precipitated in 2-propanol (EMD Millipore Inc) at −20°C overnight and centrifugation at 16 000 *g* at 4°C for 45 minutes resulted in an RNA containing pellet. Pellets were washed twice with 75% cold ethanol and dissolved in MilliQ. RNA concentrations and purity were measured using the Varioskan Flash (Thermo Scientific).

2.5 | cDNA synthesis and real-time quantitative PCR analysis

To generate cDNA, the Quantitect Reverse Transcription kit (Qiagen) was used according to the manufacturer's protocol. In short, DNAse (gDNA wipe out buffer, Qiagen) was added to ~500 ng of RNA and activated at 42°C for 2 minutes. The RNA was converted to cDNA in a 10 µL reaction mix that contained reverse transcriptase enzyme, reverse transcriptase buffer, random primers (hexanucleotides), and oligo-dTs (all Qiagen) at 42°C for 30 minutes followed by 3 minutes at 95°C. cDNA was diluted 10x in MilliQ and 1 µL was used for real-time qPCR analysis in a mix containing 1 µL of primer mix (final concentration of 0.1 µmol/L for forward and reverse primer), 5 µL of FastStart Universal SYBR Green Master mix (ROX) (Roche), and 3 µL of MilliQ. The reaction mix was added to a 96 or 384 plate and amplification of the product was measured after incubation steps at 50°C for 2 minutes, and 95°C for 10 minutes, during 40 PCR cycles (95°C for 15 seconds and 60°C for 1 minutes) using a QuantStudio 6 Flex Real-Time PCR System (Applied Biosystems). A dissociation curve was generated afterwards by ramping the temperature from 60°C to 95°C to determine the specificity of the PCR product. For detection of the GFAP isoforms the following primers were used: pan GFAP forward primer 5′-GACCTGGCCACTGTGAGG-3′, reverse primer 5′-GGCTTCATCTGCTTCCTGTC-3′, GFAPα forward primer 5′-TAGGCTCTCTCTGCTCGGTT-3′, reverse primer 5′-GAGGGCGATGTAGTAGGTGC-3′, and GFAPµ forward primer 5′-TGGCCACTGTGAGGCAGAAGAAG-3′, reverse primer 5′-TCATGCATGTTGCTGGACGC-3′. To determine specific amplification of the GFAPµ products of the qPCR, products were separated by electrophoresis in an 8% acrylamide gel made in TBE Buffer (18 mmol/L tris [hydroxymethyl]-aminomethane, 17.8 mmol/L boric acid, and 0.4 mmol/L EDTA pH 8.0 in MilliQ), stained using SYBR Safe DNA Gel Stain (Invitrogen) and imaged using an E-Gel Imager System with Blue Light Base (Life Technologies).

2.6 | Plasmid construction

Using two different primer sets, GFAP exon 1 and GFAP exon 3 CDS sequences were generated by PCR from pcDNA3.1 containing full length GFAP cDNA as a template (1 µg plasmid DNA, 10 pmol/µL forward and reverse primer, PFU buffer, PFU enzyme, 10 mmol/L dNTPs; annealing at 62°C, elongation for 5 minutes). Products were separated using gel electrophoreses and correct size products were isolated using a gel extraction kit according to the manufacturer's protocol. Exon 1 was digested at its 5′ using *Hin*dIII and exon 3 was digested at its 3′ using *Bam*HI (3 hours at 37°C). Exon 1 and exon 3 digestion products were purified using the High pure PCR product purification kit (Roche, Basel, Switzerland) according to the manufacturer's protocol. An overnight blunt ligation was induced for the 5′ of exon 1 and the 3′ of exon 3 (5 U T4 DNA ligase [Roche]) at room temperature. *Hin*dIII and *Bam*HI were again used to digest pcDNA3.1 (3 hours at 37°C) and the digestion product was separated using gel electrophoreses, isolated, and purified as described above. Exon 1 and exon 3 were ligated in pcDNA3.1 overnight at room temperature. The correct sequence was verified by sequencing (Macrogen, Amsterdam). To generate plasmid DNA containing GFAPµ cDNA and an upstream sequence encoding 20 amino acids that is recognized by the biotinylating enzyme BirA, pcDNA3.1-GFAPµ was digested using *Hind*III. The double stranded biotin-tag oligo was digested with *Hind*III as well and ligated into the pcDNA3.1-GFAPµ plasmid. The orientation of the biotin-tag was verified by sequencing (Macrogen, Amsterdam).

2.7 | Transfection

For immunostaining, cells were plated on laminin-coated coverslips in a 24-well plate at a density of 2×10^4 cells per well (SW13.Vim-, and SW13.Vim + cells) or 5×10^3 cells per well (U251-MG cells). For western blot analysis, cells were plated in a 6-well plate at a density of 5×10^5 cells per well (293T cells). Cells were transfected with empty pcDNA3.1 (mock), pcDNA3.1-GFP (GFP), pcDNA3.1-GFAPμ (GFAPμ), pcDNA3.1-bio-GFAPμ (bio-GFAPμ), pcDNA3.1-bio-GFAPα (bio-GFAPα), and/or pCI-neo-BirA (BirA) using polyethyleneimine (166 ng/mL final concentration). A total of 1 μg (immunocytochemistry) or 2.5 μg plasmid DNA (western blot) was transfected. Total transfected plasmid DNA concentrations were equal between conditions within the same experiment. Expression of plasmid DNA was allowed for 3 to 5 days depending on the experiment before cells were fixed in 4% paraformaldehyde (PFA) in phosphate buffer saline (PBS, pH 7.2) for immunostaining or cell pellets were harvested for western blot analysis.

2.8 | Immunocytochemistry

Coverslips with cells were incubated in blocking buffer (50 mmol/L Tris pH 7.4, 150 mmol/L NaCl, 0.25% (w/v) gelatin, and 0.5% triton X-100) at room temperature for 15 minutes, followed by an overnight incubation with the primary antibody in blocking buffer at 4°C. Coverslips were washed in PBS, incubated in secondary antibody in blocking buffer at room temperature for 1 hour, washed again in PBS, dipped in MilliQ, and mounted in Mowiol (0.1 mol/L Tris-HCl pH 8.5, 25% glycerol, 10% Mowiol [Calbiochem, Merck Millipore, Darmstadt, Germany]). To counterstain the nuclei of the cells, Hoechst (1:1000, 33 528, Thermo Fisher Scientific) was used and co-incubated with secondary antibodies. To label biotinylated proteins, fluorescently labeled streptavidin (1:1400 Alexa Fluor 488, Jackson Immuno Research) was co-incubated. Immunofluorescent images were taken using a Zeiss Axioscope.A1 microscope. Table 1 provides a list of antibodies used in this study.

2.9 | Western Blot analysis

Cell pellets were resuspended in suspension buffer (0.1 mol/L NaCl, 0.01 mol/L Tris-HCl pH 7.6, 0.001 mol/L EDTA, and cOmplete EDTA-free protease inhibitor cocktail [Roche]) and lysed in 2x SDS loading buffer (100 mmol/L Tris pH 6.8, 4% SDS, 20% glycerol, 5% 2-mercaptoethanol, and bromophenol blue). Samples were heated at 95°C for 5 minutes after which the DNA was sheared using a 25 gauge

TABLE 1 List of antibodies

Antibody	Product code, company	Dilution western blot	Dilution immunocytochemistry
Rabbit anti-GFAP (panGFAP)	#Z0334, Dako (Agilent), Santa Clara, CA, USA	1:50,000	1:4,000
Goat anti-GFAP N-18 (N-term)	sc-6171, Santa Cruz, Dallas, Texas, USA	1:1,000	1:1,000
Chicken anti-Vimentin	AB5733, Chemicon, Temecula, California	—	1:4,000
Donkey anti-rabbit Cy3	Jackson Immuno Research, West Grove, PA, USA	—	1:1,000
Donkey anti-goat 488	Jackson Immuno Research, West Grove, PA, USA	—	1:1,000
Donkey anti-rabbit IRdye800	Jackson Immuno Research, West Grove, PA, USA	1:5,000	—
Donkey anti-goat AF647	Jackson Immuno Research, West Grove, PA, USA	1:2,000	—
Donkey anti-chicken Dylight488	Jackson Immuno Research, West Grove, PA, USA	1:2,000	—

needle. Samples were loaded on a 15% SDS-PAGE gel and proteins were separated by electrophoresis. Proteins were blotted on a 0.45 µmol/L pore size nitrocellulose membrane (GE Healthcare) using a Transblot SD semi-dry transfer system (Bio-Rad) system for 1 hour. Blots were incubated in blocking buffer (50 mmol/L Tris pH 7.4, 150 mmol/L NaCl, 0.25% (w/v) gelatin, and 0.5% triton X-100) and incubated in primary antibody in blocking buffer at 4°C O/N. Blots were washed three times in TBS-T (100 mmol/L Tris-HCl pH 7.4, 150 mmol/L NaCl, and 0.2% Tween-20) and incubated in secondary antibody in blocking buffer at room temperature for 1 hour. To label biotinylated proteins, blots were incubated with fluorescently labeled streptavidin (1:2000 Alexa Fluor Cy5, Jackson Immuno Research). Blots were washed three times in TBS-T and ones in milliQ before blots were scanned using the Odyssey CLx Western Blot Detection System (LI-COR Biosciences). Table 1 provides a list of used antibodies.

2.10 | Statistics

To determine differential expression of GFAPµ the data were tested for a normal distribution and normality of variances using the Shapiro-Wilk test and Levene's test. A one-way ANOVA or Kruskal-Wallis test was performed dependent on the distribution of the data followed by a post hoc Tukey's honestly significant difference tests or Nemenyi tests, respectively. All analyses were performed using R software (version 3.4.3) and the PMCMR package (version 4.3). Survival analysis (including progression free survival) was performed using the Survival package (version 2.41-3). Kaplan-Meier survival curves were compared using a log-rank regression analysis.

3 | RESULTS

3.1 | Differential expression of a short GFAP transcript in glioma subtypes

The analysis of RNA sequencing data of glioma patients from The Cancer Genome Atlas (TCGA) (Table S1) revealed the expression of a third GFAP isoform in addition to the well-known GFAPα and GFAPδ isoforms.[27] The CDS of this third GFAP isoform, GFAPµ, consisted of only exon 1 and exon 3 of the GFAP gene according to the RNA sequencing transcript annotation file (Table S2) and the Ensembl database (GFAP-202, www.ensembl.org). GFAPµ was expressed in astrocytoma grade II, III, and IV (Figure 1A) and the expression was significantly decreased in grade IV astrocytoma patients. This expression pattern follows the decrease of the canonical GFAPα isoform in high-grade astrocytoma as we previously reported.[27] However, the overall expression level of GFAPµ was about 5000 times lower. The GFAPµ expression levels did not correlate with patient prognosis within grade II, III, or IV astrocytoma (data not shown).

Recently, the World Health Organization has changed the glioma classification system (WHO 2016) based on additional molecular tumor characteristics. Expression of GFAPµ in these glioma subtypes is shown in Figure 1B. GFAPµ was higher expressed in low-grade IDH1 mutated and IDH1 wild-type tumors without a 1p/19q deletion compared to grade IV IDH1 mutated and wild-type tumors. GFAPµ expression in IDH1-mutated tumors with a 1p/19q deletion was lower compared to low-grade IDH1 mutated and wild-type tumors as well. Within these glioma subtypes, GFAPµ did not have a significant prognostic value for patients either (data not shown).

3.2 | GFAPµ mRNA expression in human brain tissue and glioma cells

Generation of the GFAPµ transcript must be proceeded by a new alternative splicing event of the GFAP gene that leads to skipping of exon 2. Skipping of exon 2 induces a frame-shift and PTC in exon 3 of the resulting transcript (Table S2 and Table S3). The CDS of GFAPµ, therefore, only consists of 540 base pairs (bp), which is less than half of the 1299 bp CDS of GFAPα (Figure 2B, Table S2). To determine if the skipping of GFAP exon 2 is an alternative splicing event that is observed more often, we performed qPCR analysis on different samples using GFAPµ-specific primers followed by gel electrophoresis (Figure 1C-F). The forward primer was designed to bind to the 3′ end of exon 1 and two nucleotides at the 5′ end of exon 3 (thus spanning exon 1 and 3). The reverse primer was designed to bind exon 3 downstream of the forward primer to generate a 252 bp product. Figure 1C lane 2 shows that this primer pair could also amplify GFAPα cDNA that contains exon 1, 2 and 3. However, the size of the product is longer (331 bp) as it includes exon 2. Amplification of GFAPµ generated a 252 bp product (Figure 1C lane 3). Figure 1C, lane 5 and 6 show that a 252 bp GFAPµ product was detected in RNA isolated from both healthy human brain tissue and from the human U251-MG glioma cell line. Figure 1E lane 3 and Figure 1F lane 3 show that when combining GFAPα cDNA and GFAPµ cDNA, the amplification of the 252 bp GFAPµ product was preferred. GFAPµ was detected in 2 human spinal cord tissue samples (Figure 1D), 2 out of 3 human brain samples (Figure 1E, lane 5-7), and in different U251-MG glioma clonal cell lines (Figure 1E, lane 8-13). In addition, GFAPµ was detected in two primary glioma cell cultures (Figure 1F, lane 5-8). GFAPµ was not detected in ihNSCs (Figure 1C) or adult neural stem cells isolated from human postmortem tissue that did express pan GFAP (data not shown). These results suggest that the

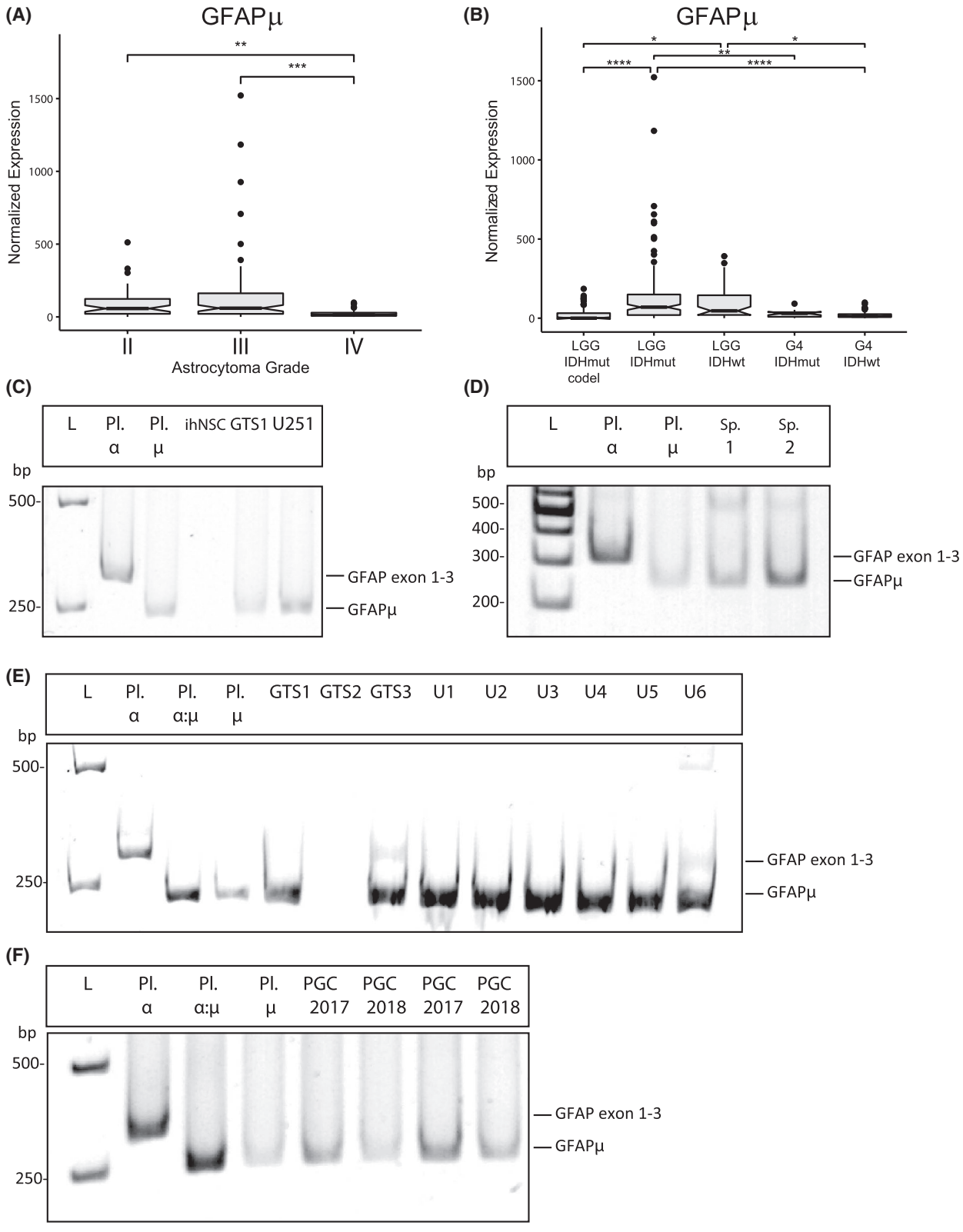

FIGURE 1 GFAPμ expression in glioma subtypes, glioma primary cells and cell lines, and in healthy brain tissue. A and B, Normalized expression of a new GFAP isoform (GFAPμ) in astrocytoma of grade II, III and IV (WHO 2007) and in different glioma subtypes (WHO 2016). Expression levels were obtained from RNAseq level 3 released normalized isoform expression data of the TCGA database (*LGG* = grade II and III glioma, *G4* = grade IV glioma, *IDHmut* = IDH1 mutation, *codel* = 1q19p co-deletion, *whiskers*: ±1.5 × IQR; *notch*: 95% CI). C-F, Images of qPCR products separated on an 8% acrylamide gel by electrophoreses. Products of 252 bp are generated from GFAPμ transcripts. Products of 313 bp are generated from GFAP transcripts that contain exon 1, 2, and 3 (*L* = ladder, *Pl. α* = GFAPα plasmid cDNA, *Pl. μ* = GFAPμ plasmid cDNA, *ihNSC* = immortalized adult human neural stem cells, *GTS1-3* = 3 different human temporal cortex samples, *Sp 1 and 2* = 2 different human spinal cord samples, *U251* = U251-MG glioma cells, *U1-U6* = different U251-MG clonal cell lines, PGC = primary glioma cells isolated in 2017 and 2018). **P* < .05, ***P* < .01, ****P* < .001, *****P* < .0001

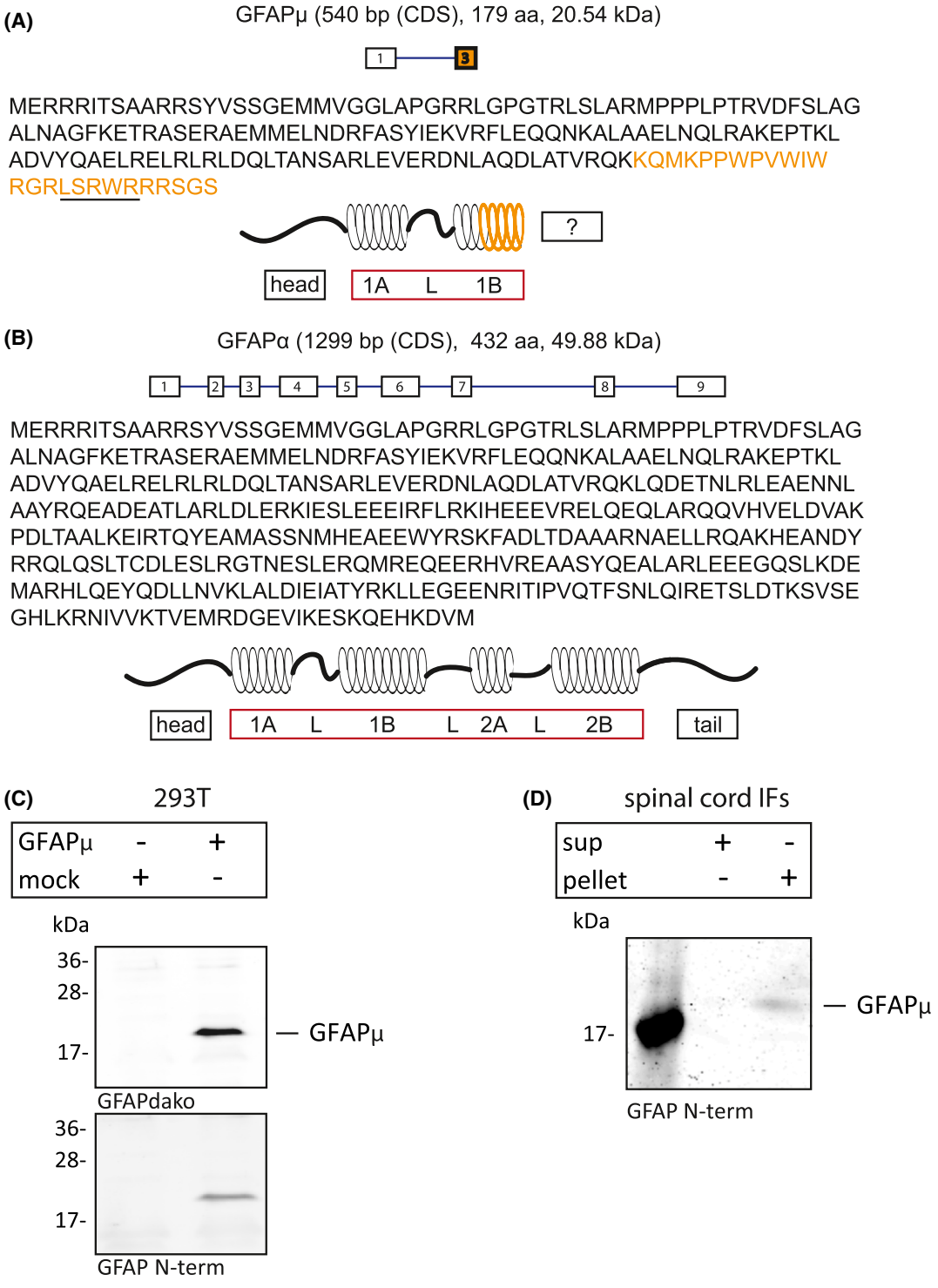

FIGURE 2 GFAPμ characteristics and western blot analysis. A and B, Characteristics of GFAPμ and the canonical GFAPα isoform transcripts and proteins and a hypothesized protein structure of GFAPμ (*1A = helical coiled-coiled segment 1A, L = Linker segments, 1B = helical coiled-coiled segment 1, 2A = helical coiled-coiled segment 2A, 2B = helical coiled-coiled segment 2B*). The underlined sequence indicates the peptide that was found in a human proteomics study.[34] C, Western blot analysis of whole lysates of GFAPμ and mock transfected 293T cells. Western blots were stained with two different GFAP antibodies that recognize a protein sequence encoded by exon 1 (top) and the N-terminal head of GFAP (bottom). D, Western blot of intermediate filament protein isolated from the human spinal cord. The blot was stained with a GFAP antibody that recognizes the N-terminal head of the GFAP protein (*L = protein ladder*)

skipping of exon 2 is a common GFAP alternative splicing event that generates stable GFAPμ mRNA molecules in glioma and in the healthy central nervous system.

3.3 | GFAPμ is translated into a 21 kDa sized protein

The annotation of a unique peptide (Figure 2A, underlined sequence) that specifically aligns to the GFAPμ protein sequence was found in a human proteomics study[34] and suggested that GFAPμ is a protein coding alternative splice variant. The data of this study are deposited in a protein database (proteomicsdb.org) where GFAPμ is annotated as GFAP-B1DIR4. Comparison of the canonical isoform GFAPα (Figure 2B) and GFAPμ (Figure 2A) protein sequences showed that the predicted GFAPμ protein lacks a large part of the IF rod domain and its entire tail. To confirm translation of the GFAPμ CDS and stable expression of the protein, we expressed GFAPμ cDNA (Table S2) in 293T cells. Western blotting of proteins isolated from GFAPμ and mock transfected cells (Figure 2C) confirmed the expression of a ~21 kDa protein recognized by two different GFAP antibodies. Both antibodies recognize the GFAP N-terminal region that is present in GFAPμ. In 293T cells, which have undetectable endogenous GFAP expression, a clear and strong GFAPμ band is visible in the transfected cells (Figure 2C). This confirms that GFAPμ cDNA can translate into a stable protein. Interestingly, on a western blot of IF proteins isolated from the human spinal cord, a ~21 kDa size protein was detected by the GFAP N-terminal antibody (Figure 2D), suggesting translation and stable protein expression of the endogenous GFAPμ transcript.

3.4 | Limited GFAPμ self-assembly and de novo filament formation

We continued to investigate the behavior of the GFAPμ protein in different cellular environments. GFAP variants lacking essential domains of the N-terminal head, rod or C-terminal tail are assembly compromised and form aggregates in the absence of other IF proteins with which they can co-assemble.[11,32,35-37] To determine whether GFAPμ is capable of de novo filament formation in the absence of other IF proteins, we used the human adrenal carcinoma-derived cell line SW13 devoid of vimentin (SW13.Vim-) and other cytoplasmic IFs. As described in previous studies,[36,38] the canonical splice variant GFAPα forms a filamentous network in these cells (Figure 3A). Immunostainings of mock and GFAPμ transfected SW13.Vim- cells for two different GFAP antibodies which recognize GFAPμ are shown in Figure 3B-F. In most cells, GFAPμ expression led to diffuse non-filamentous GFAP immunostaining with small and bright GFAP aggregates throughout the cell's cytoplasm (Figure 3C,D) and/or larger (peri-)nuclear aggregations (Figure 3E). A rare observation of filament formation is shown in Figure 3F where GFAP positive filament-like bundles were seen around the nuclei of these cells. However, as these cells seem to be dividing this might be a cellular state-specific staining pattern and no direct evidence of GFAPμ self-assembly. Confocal imaging showed that in some cells the aggregated structures in the cell periphery were short and thick filament-like structures (Figure 3G,H). Furthermore, Figure 3H shows that aggregates did not overlap with Hoechst staining but were present in the peri-nuclear regions and most likely within the nuclear invaginations.[39] These results do not provide evidence for the ability of GFAPμ to self-assemble into filaments.

3.5 | GFAPμ expression patterns in the presence of the GFAP assembly partner vimentin

GFAP mutants or isoforms that lack essential domains to self-assemble into filaments can disrupt the existing IF network or make use of IF assembly partners that are present to co-assemble.[11,32,35-37] To determine the behavior of GFAPμ in the presence of the known GFAP assembly partner vimentin, GFAPμ was expressed in SW13.Vim + cells (Figure 4). Co-immunostaining for vimentin and GFAP showed different patterns of IF expression. In some un-transfected control cells, cross-reactivity of the GFAP Dako antibody with vimentin was observed (Figure 4A), but immunostaining intensity was much stronger and did not co-localize with vimentin in GFAPμ transfected cells (Figure 4B-I). In Figure 4B,C, cells with diffuse GFAP expression are shown that contained brighter aggregated GFAP structures near the nucleus. In these cells, vimentin was mainly present near the nucleus as well and the brighter filamentous structures as seen in most control cells were absent (Figure 4B). However, this vimentin staining pattern was not unique for GFAPμ positive cells and was seen in some un-transfected controls (Figure 4A,B,D) as well. In addition, Figure 4D shows similar diffuse GFAP staining and peri-nuclear aggregates, whereas vimentin positive structures were brighter and filamentous. Confocal imaging shows that the GFAP aggregates localize to the intact vimentin network (Figure 4E). The GFAP aggregation observed was similar to the in Figure 3G,H described small thick filamentous structures. Furthermore, some cells contained larger peri-nuclear aggregates of both GFAP and vimentin (Figure 4F). A fourth common pattern is shown in Figure 4G,H in which a low cytoplasmic GFAP staining was seen together with bright small GFAP positive aggregates and an intact filamentous vimentin IF network. In some

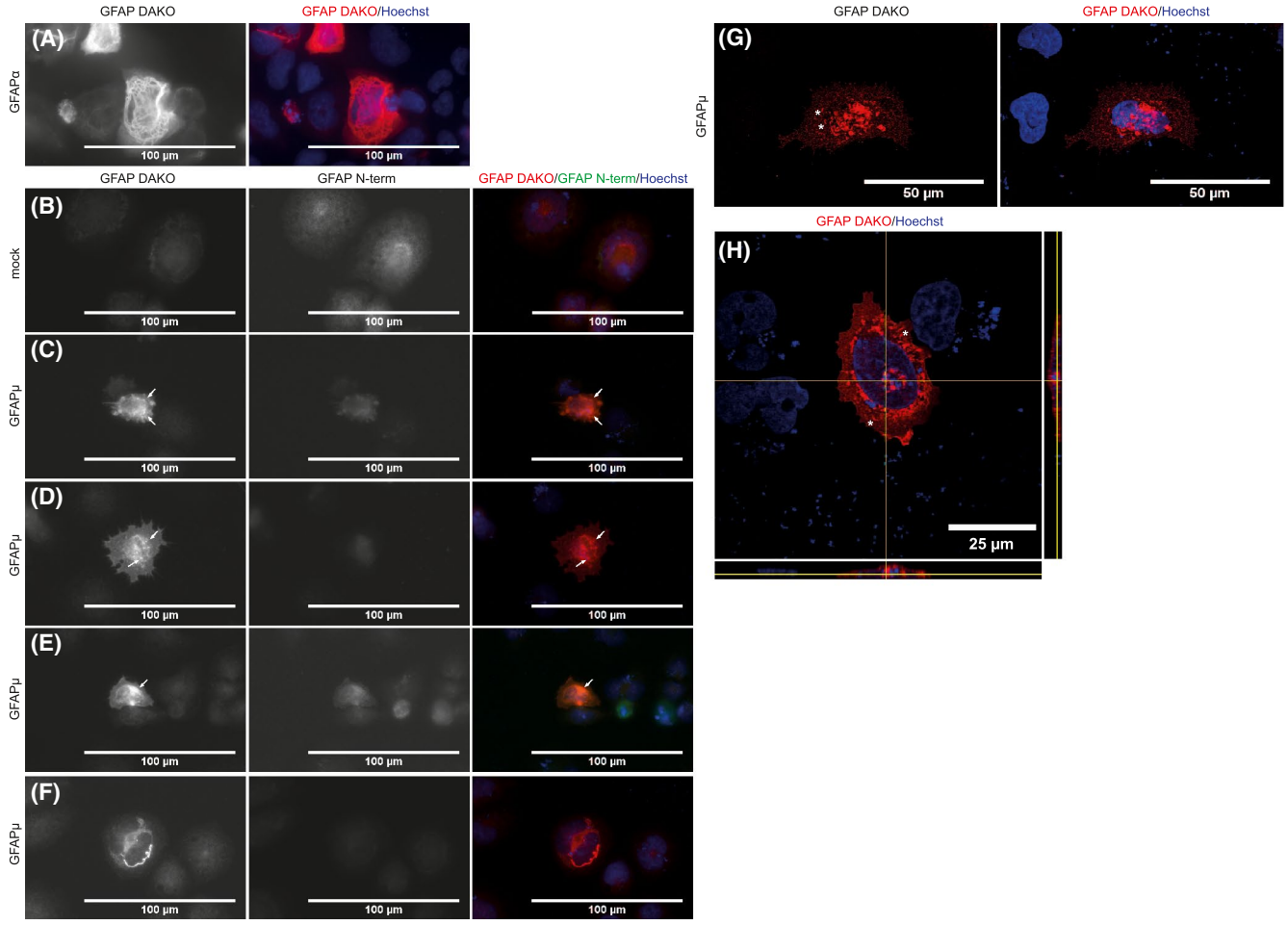

FIGURE 3 GFAPµ staining patterns in SW13.Vim- cells. Immunostaining images of GFAPα (A), mock (B), and GFAPµ (C-H) transfected SW13.Vim- cells. A GFAPα transfected cells stained using a GFAP (Dako) antibody. B-H Mock and GFAPµ transfected cells stained using two different GFAP antibodies (GFAP Dako [left], GFAP N-term [middle]) and Hoechst (right). Diffuse GFAPµ expression in small bright and larger peri-nuclear aggregates (arrows indicate aggregates) (C and D). A pattern of diffuse GFAPµ expression and large peri-nuclear aggregation (arrows indicate aggregates) (E). Filamentous expression patterns of GFAPµ around the nuclei (F). Confocal images of thick filamentous structures (G) and peri-nuclear GFAP aggregates (H). Asterisks (*) indicate short and thick filament-like structures

cases, the aggregates lined up along the vimentin network. These results do not provide clear evidence for GFAPµ-induced disruption of the vimentin IF network or vimentin-GFAPµ co-assembly.

3.6 | GFAPµ expression disrupts the endogenous GFAP network in glioma cells

To determine effect of GFAPµ expression on the GFAP-containing IF network of glioma, we expressed GFAPµ in the U251-MG glioma cells (Figure 5). These cells express endogenous GFAP, vimentin, nestin, and synemin.[28] Small and bright GFAP positive aggregates were observed upon GFAPµ expression (Figure 5B,C). Similar to the observations in SW13.Vim + cells (Figure 4), the aggregates did not contain vimentin indicating that GFAPµ does not affect vimentin filaments.

The GFAP antibody used here recognizes all GFAP isoforms, including GFAPµ (Figure 5). Therefore, GFAPµ protein was biotinylated to assess the effect of GFAPµ on the endogenous GFAP network of glioma cells without the availability of a GFAPµ-specific antibody. We generated a construct that encodes GFAPµ protein with an N-terminal 12 amino acid long tag (bio-GFAPµ) that is recognized and biotinylated by the E. coli biotin ligase BirA. Streptavidin labeling of cells co-transfected with BirA and bio-GFAPµ specifically visualized bio-GFAPµ protein. Co-localization analysis of streptavidin and GFAP immunostaining indicated where and how GFAPµ protein is expressed in the cell.

Bio-GFAPµ aggregated in all bio-GFAPµ expressing U251-MG cells (Figure 6). Intense streptavidin labeling of aggregates in bio-GFAPµ and GFP co-transfected cells (Figure 6A) and GFAP positive aggregates in bio-GFAPµ transfected cells (Figure 6C-F) showed that the GFAP positive aggregates contain GFAPµ protein. Confocal imaging

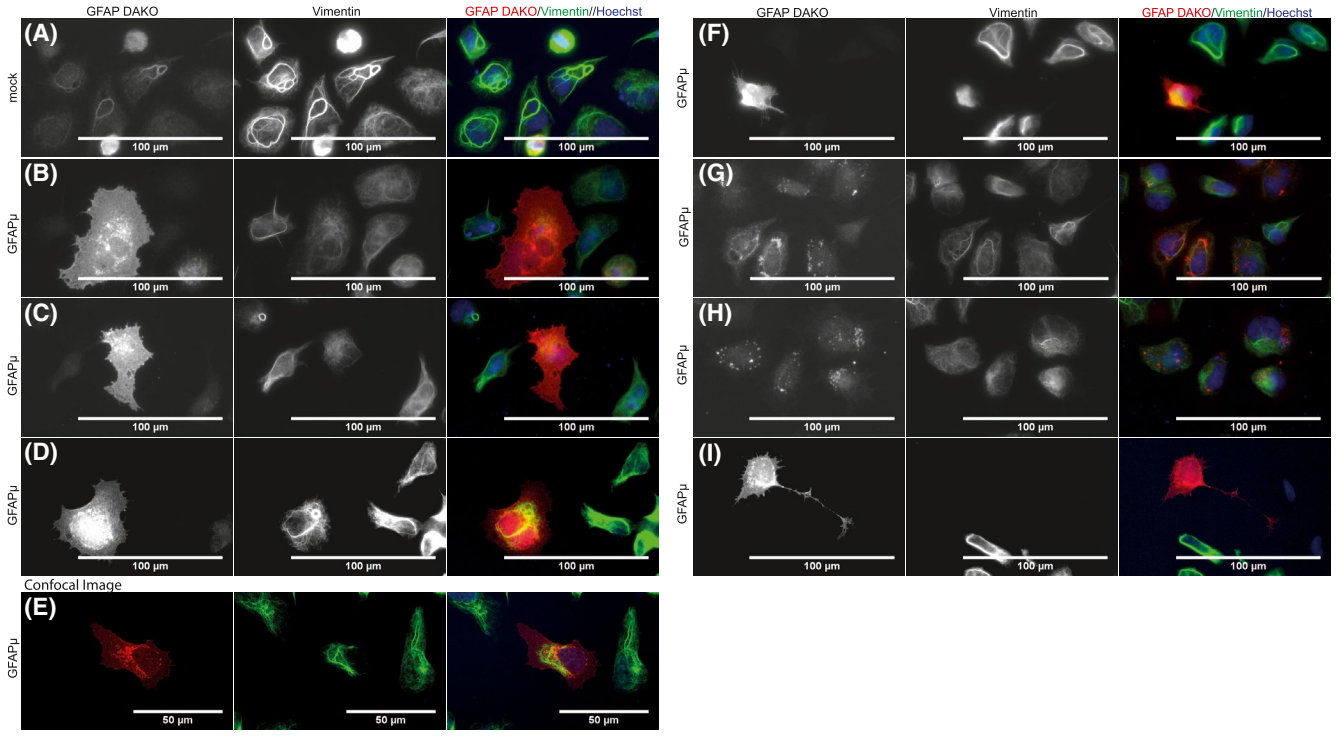

FIGURE 4 GFAPμ staining patterns in SW13.Vim + cells. Immunostaining of mock transfected (A) and GFAPμ transfected SW13.Vim+ (B-I) cells for GFAP (Dako) and vimentin. A Mock transfected cells. Vimentin staining showed bright and thick filament bundles as well as thinner filamentous, less bright, structures. Some cross-reactivity of the GFAK Dako antibody is observed. B, C Cells with diffuse GFAP staining and small (B) or big peri-nuclear (C) aggregates and localization of vimentin thin filamentous structures to the nucleus. D Cells with diffuse GFAP immunostaining including large aggregation near the cell's nucleus. In these cells, vimentin localized to the cell's nucleus in thick and bright filament bundles. E Confocal image of a cell with GFAP positive aggregates that localize to the vimentin intact network. F A cell with a large GFAP and vimentin positive peri-nuclear aggregate. G, H Cells in which small GFAP aggregates are present that seemed to align alongside bright vimentin filamentous structures

showed the presence of GFAP positive and streptavidin negative aggregates as well, indicating that GFAPμ disrupts the endogenous GFAP network (Figure 6E,F, indicated with arrows). To exclude an effect of N-terminal biotin on the assembly of GFAP IFs, bio-GFAPα and BirA were co-expressed in SW13.Vim- cells. Bright streptavidin fluorescence of GFAP filaments similar to filaments observed upon the expression of unlabeled GFAPα were observed (Figure S1A, B). We, therefore, excluded the possibility of a sole effect of biotin to the disruption of the endogenous GFAP network and attribute our observations to the expression of GFAPμ. Western blot analysis of total GFAP protein levels upon expression of (bio-)GFAPμ and (bio-)GFAPα cDNA further showed that GFAPμ-induced aggregates were an isoform-specific observation and was not due to higher total GFAP protein levels (Figure S1C). Interestingly, when bio-GFAPμ was co-transfected at different ratios with GFAPα in U251-MG cells, reducing the relative expression of bio-GFAPμ, disruption of the endogenous GFAP network was rare, and bio-GFAPμ integration into the GFAP network was observed (Figure S2).

4 | DISCUSSION

The process of alternative splicing is essential for the diversification of cellular phenotype and function. Differences in RNA isoform expression between tissue types and alterations in various types of cancers have been identified by RNA sequencing.[18-20] In glioma, alterations in the expression of the type III IF GFAP isoforms GFAPα and GFAPδ have functional implications for the malignant behavior of tumor cells.[6,27-29,35] In this study, the analysis of RNA sequencing data of glioma patient material has revealed the expression of another and new GFAP isoform in glioma, GFAPμ. The GFAPμ transcript was detected in different glioma subtypes by RNA sequencing and was significantly decreased in grade IV glioma. The expression of GFAPμ mRNA, a product of GFAP exon 2 skipping which results in a PTC in exon 3, was confirmed by qPCR analysis in healthy brain tissue, spinal cord tissue, glioma cell lines, and primary glioma cells. We here provide evidence for a new GFAP alternative splicing event observed in glioma and in the healthy brain that results in the expression of GFAPμ.

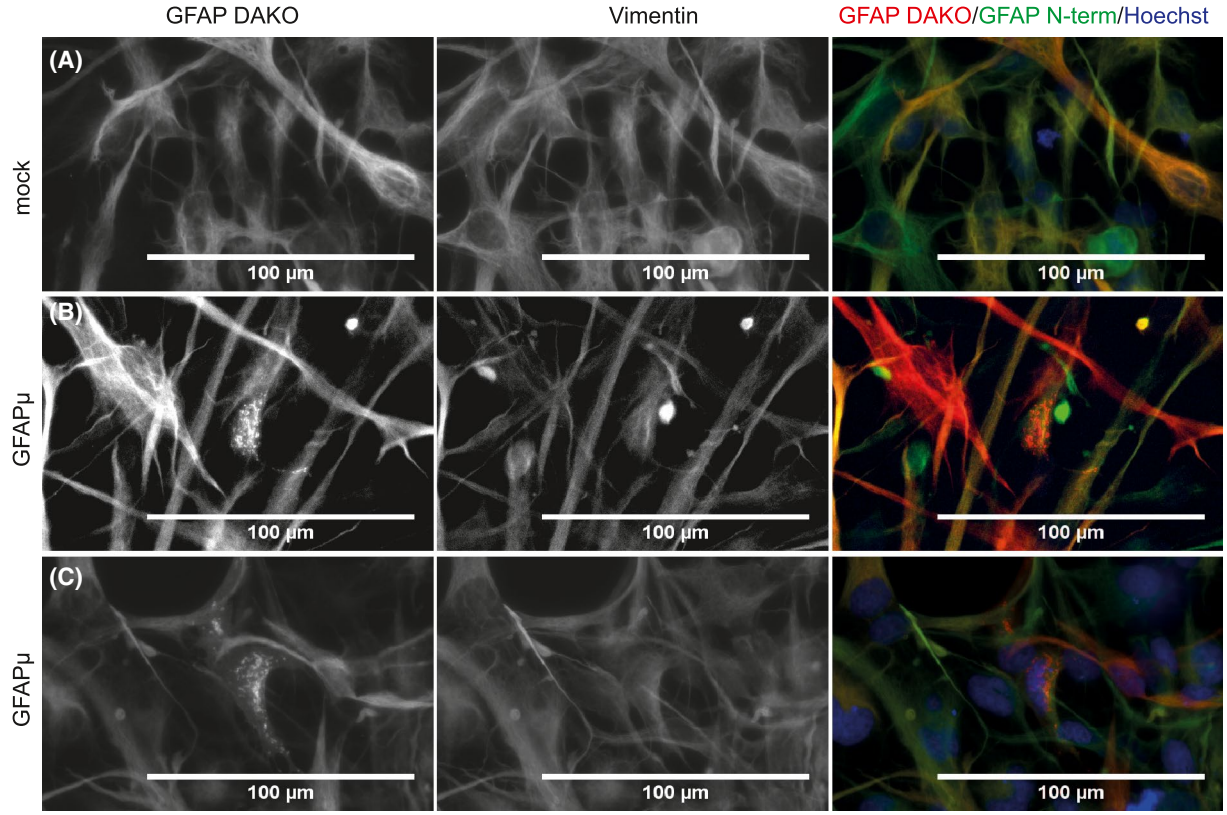

FIGURE 5 GFAPμ staining patterns in U251-MG cells. Immunostainings of mock (A) and GFAPμ (B and C) transfected U251-MG cells. U251-MG cells were stained for GFAP Dako (left), vimentin (middle), and Hoechst. A Immunostaining of U251-MG mock transfected cells showed a characteristic GFAP and vimentin intermediate filament network. B and C, GFAPμ transfected cells contained GFAP positive small and bright aggregates that are negative for vimentin

The detection of a GFAPμ-specific peptide in a human proteomics study[34] and a ~21 kDa GFAP protein in the IF fraction of proteins isolated from the human spinal cord in this study, provide evidence for translation of the transcript and endogenous expression of GFAPμ protein. Despite these observations, it is important to note that the GFAPμ transcript might be targeted by the process of nonsense-mediated RNA decay.[25] As GFAPμ contains a PTC in close proximity to an exon-exon junction (51 bp for GFAPμ), it might be recognized as an error during the translation process and being targeted for degradation, as was predicted for this transcript in the Ensembl database (GFAP-202, www.ensembl.org). As most PTC-bearing mRNAs are downregulated by the enhancement of splicing of the canonical transcript,[40] and GFAPμ was detected at ~5000 times lower levels compared to GFAPα in RNA sequencing data of TCGA, this possibility should not be neglected. However, as evidence supports endogenous expression of GFAPμ protein, it is more likely that an alternative polyadenylation signal within the 3′UTR of GFAPμ exon 3 is recognized resulting in removal of the exon 3 to exon 4 junction from the transcript and the stable translation of GFAPμ.

We further showed that inducing the expression of the GFAPμ CDS generated a ~21 kDa protein. This short GFAPμ protein behaved as expected from its sequence and had a low capacity to self-assemble and formed aggregates in the absence of other GFAP proteins. We observed some short and thick filament-like structures in the absence of other cytoplasmic IFs that could be evidence of filament precursors called squiggles.[41] These structures form at the cell periphery and when they fail to integrate into a network they aggregate. In glioma cells, the induced expression of GFAPμ disrupted the existing GFAP IF network. The presence of GFAP positive and biotin-negative small and bright aggregates, showed that GFAPμ can induce aggregation of the endogenous GFAP network. Induced overexpression of the self-assembly incompetent GFAPδ isoform in glioma cells disrupts the IF network of glioma cells as well.[35] However, increased endogenous GFAPδ protein leaves the IF network intact and impacts glioma cell malignant behavior.[29] In these cells, higher levels of GFAPδ are observed within the IF network. As GFAPμ is expressed 5000 times lower compared to GFAPα in glioma, the induced expression levels of GFAPμ in our experiments far exceed the endogenous level. We, therefore, hypothesize that, like GFAPδ, GFAPμ can integrate into the IF network when expressed at endogenous levels and thereby contribute to the function of glioma cells. Co-expression experiments of GFAPμ at different ratios to GFAPα in glioma cells support this hypothesis.

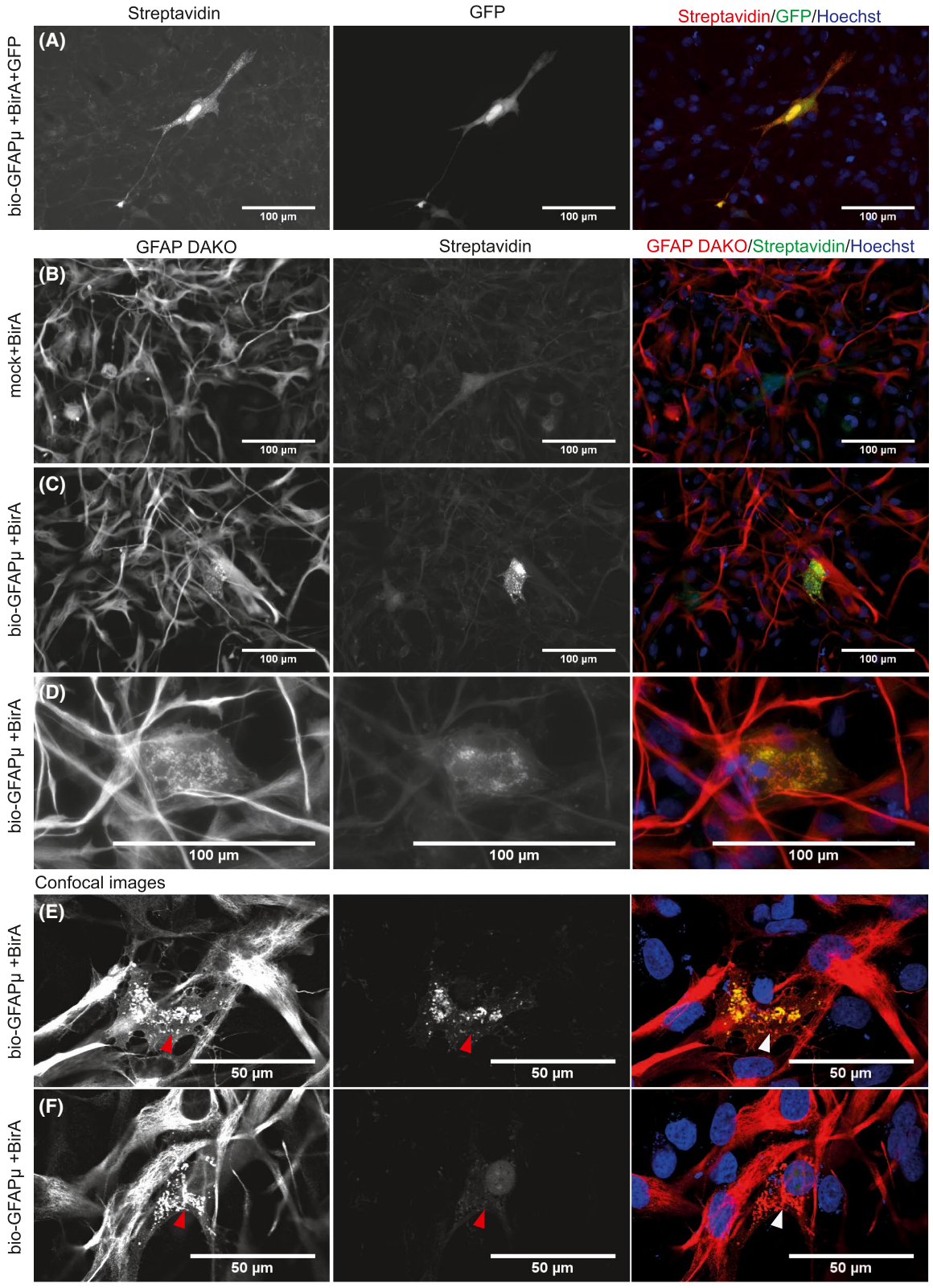

FIGURE 6 Visualization of bio-GFAPμ in the GFAPμ-induced disrupted U251-MG IF network. Immunostaining of U251-MG cells for GFAP. Biotinylated proteins were labeled with streptavidin. The nucleus was counterstained using Hoechst. A, Cells transfected with bio-GFAPμ, BirA and GFP (transfection control) and labeled for streptavidin. Streptavidin positive GFAPμ characteristic aggregates are found in the GFP positive cells. B, Control cells in which empty pcDNA3.1 was co-transfected with BirA to determine background biotin and biotinylation. C and D, GFAP immunostaining and streptavidin labeling of cells co-transfected with bio-GFAPμ and BirA show co-localization of GFAP and streptavidin in bright streptavidin positive cells. E and F, Confocal images of cells co-transfected with bio-GFAPμ and BirA that show GFAP positive and streptavidin negative (arrows) aggregates

Glioma consist of a heterogeneous population of GFAP positive cells.[6] We previously described that the increased relative expression of GFAPδ to GFAPα might distinguish a GFAP positive subpopulation of high malignant glioma cells with invasive characteristics.[6,27,29] As GFAPμ expression was decreased in high malignant glioma and absent in GFAP expressing ihNSCs and adult neural stem cells, we hypothesize that GFAPμ is expressed in lower malignant glioma and more differentiated cell types. Future studies that analyze GFAPμ expression in different types of tissue and cells and determine the functional consequences of GFAPμ expression and integration into the IF network, are needed to confirm this hypothesis.

The here reported differential expression of GFAPμ in glioma subtypes in addition to GFAPα and GFAPδ further emphasizes the importance of GFAP isoform-specific analysis in glioma diagnostics and research. GFAP alternative splicing could form an interesting therapeutic target for glioma treatment. Mechanistic knowledge on GFAP RNA processing and functional consequences of GFAP isoform-specific IF networks for glioma malignancy are needed to further evaluate this possibility.

ACKNOWLEDGMENTS

The authors thank Vanessa Marques Donega and Marjolein Sneeboer for providing us with RNA samples of primary adult neural stem cells and human brain tissue. The results shown here are in part based on data generated by the TCGA Research Network: http://cancergenome.nih.gov/. This work was supported by the Netherlands Organization for Scientific Research (NWO; VICI grant 865.09.003), the T&P Bohnenn fund, the Dutch Cancer Society (KWF 10123), and the Netherlands Brain Bank (NBB), which is supported by the Netherlands Organization for Scientific Research (NWO).

CONFLICT OF INTEREST

The authors declare no conflict of interest.

AUTHOR CONTRIBUTIONS

EJ van Bodegraven, PAJT Robe, and EM Hol designed the research; EJ van Bodegraven analyzed the data; EJ van Bodegraven, JA Sluijs, and AK Tan performed the research; EJ van Bodegraven and EM Hol wrote the paper.

ORCID

Emma J. van Bodegraven https://orcid.org/0000-0002-3796-2516
Elly M. Hol https://orcid.org/0000-0001-5604-2603

REFERENCES

1. Middeldorp J, Hol EM. GFAP in health and disease. *Prog Neurogibol*. 2011;93:421-443.
2. Hol EM, Pekny M. Glial fibrillary acidic protein (GFAP) and the astrocyte intermediate filament system in diseases of the central nervous system. *Curr Opin Cell Biol*. 2015;32:121-130.
3. Velasco ME, Dahl D, Roessmann U, Gambetti P. Immunohistochemical localization of glial fibrillary acidic protein in human glial neoplasms. *Cancer*. 1980;45:484-494.
4. Dunbar E, Yachnis AT. Glioma diagnosis: immunohistochemistry and beyond. *Adv Anat Pathol*. 2010;17:187-201.
5. Perry A, Wesseling P. Histologic classification of gliomas. In: Berger MS, Weller M, eds. *Handbook of Clinical Neurology*. Vol. 134. Elsevier; 2016:71–95.
6. van Bodegraven EJ, van Asperen JV, Robe PAJ, Hol EM. Importance of GFAP isoform-specific analyses in astrocytoma. *Glia*. 2019;67(8):1417–1433.
7. Blechingberg J, Lykke-Andersen S, Jensen TH, Jørgensen AL, Nielsen AL. Regulatory mechanisms for 3′-end alternative splicing and polyadenylation of the Glial Fibrillary Acidic Protein, GFAP, transcript. *Nucleic Acids Res*. 2007;35:7636-7650.
8. Kanski R, Sneeboer MAM, van Bodegraven EJ, et al. Histone acetylation in astrocytes suppresses GFAP and stimulates a reorganization of the intermediate filament network. *J. Cell Sci*. 2014;127:4368-4380.
9. Reeves SA, Helman LJ, Allison A, Israel MA. Molecular cloning and primary structure of human glial fibrillary acidic protein. *Proc Natl Acad Sci USA*. 1989;86:5178-5182.
10. Nielsen AL, Holm IE, Johansen M, Bonven B, Jørgensen P, Jørgensen AL. A new splice variant of glial fibrillary acidic protein, GFAPε, interacts with the presenilin proteins. *J Biol Chem*. 2002;277:29983-29991.
11. Roelofs RF, Fischer DF, Houtman SH, et al. Adult human subventricular, subgranular, and subpial zones contain astrocytes with a specialized intermediate filament cytoskeleton. *Glia*. 2005;52:289-300.
12. Zelenika D, Grima B, Brenner M, Pessac B. A novel glial fibrillary acidic protein mRNA lacking exon 1. *Brain Res Mol Brain Res*. 1995;30:251-258.
13. Blechingberg J, Holm IE, Nielsen KB, Jensen TH, Jørgensen AL, Nielsen AL. Identification and characterization of GFAPκ, a novel glial fibrillary acidic protein isoform. *Glia*. 2007;55:497-507.
14. Hol EM, Roelofs RF, Moraal E, et al. Neuronal expression of GFAP in patients with Alzheimer pathology and identification of novel GFAP splice forms. *Mol Psychiatry*. 2003;8:786-796.
15. Helman G, Takanohashi A, Hagemann TL, et al. Type II Alexander disease caused by splicing errors and aberrant overexpression of an uncharacterized GFAP isoform. *Hum Mutat*. 2020;41(6):1131–1137.
16. Hol EM, Capetanaki Y. Type III intermediate filaments desmin, glial fibrillary acidic protein (GFAP), vimentin, and peripherin. *Cold Spring Harb Perspect Biol*. 2017;9:a021642.
17. Ameur A, Zaghlool A, Halvardson J, et al. Total RNA sequencing reveals nascent transcription and widespread co-transcriptional splicing in the human brain. *Nat Struct Mol Biol*. 2011;18:1435-1440.
18. Elkon R, Ugalde AP, Agami R. Alternative cleavage and polyadenylation: extent, regulation and function. *Nat Rev Genet*. 2013;14:496-506.
19. Bentley DL. Coupling mRNA processing with transcription in time and space. *Nat Rev Genet*. 2014;15:163-175.
20. Herzel L, Ottoz DSM, Alpert T, Neugebauer KM. Splicing and transcription touch base: co-transcriptional spliceosome assembly and function. *Nat Rev Mol Cell Biol*. 2017;18:637-650.

21. Dvinge H, Bradley RK. Widespread intron retention diversifies most cancer transcriptomes. *Genome Med*. 2015;7:9.
22. Lee SC-W, Abdel-Wahab O. Therapeutic targeting of splicing in cancer. *Nat Med* 2016;22:976-986.
23. Morris AR, Bos A, Diosdado B, et al. Alternative cleavage and polyadenylation during colorectal cancer development. *Clin Cancer Res*. 2012;18:5256-5266.
24. Chen L, Tovar-Corona JM, Urrutia AO. Increased levels of noisy splicing in cancers, but not for oncogene-derived transcripts. *Hum Mol Genet*. 2011;20:4422-4429.
25. Hug N, Longman D, Cáceres JF. Mechanism and regulation of the nonsense-mediated decay pathway. *Nucleic Acids Res*. 2016;44:1483-1495.
26. Fu Y, Sun Y, Li Y, et al. Differential genome-wide profiling of tandem 3' UTRs among human breast cancer and normal cells by high-throughput sequencing. *Genome Res*. 2011;21:741-747.
27. Stassen OMJA, van Bodegraven EJ, Giuliani F, et al. GFAPδ/GFAPα ratio directs astrocytoma gene expression towards a more malignant profile. *Oncotarget*. 2017;8:88104-88121.
28. Moeton M, Kanski R, Stassen OMJA, et al. Silencing GFAP isoforms in astrocytoma cells disturbs laminin-dependent motility and cell adhesion. *FASEB J*. 2014;28:2942-2954.
29. van Bodegraven EJ, van Asperen JV, Sluijs JA, et al. GFAP alternative splicing regulates glioma cell-ECM interaction in a DUSP4-dependent manner. *FASEB J Off Publ Fed Am Soc Exp Biol*. 2019;33:12941-12959.
30. The Cancer Genome Atlas Research Network. Comprehensive, integrative genomic analysis of diffuse lower-grade gliomas. *N Engl J Med*. 2015;372:2481-2498.
31. van Strien ME, Sluijs JA, Reynolds BA, Steindler DA, Aronica E, Hol EM. Isolation of neural progenitor cells from the human adult subventricular zone based on expression of the cell surface marker CD271. *Stem Cells Transl Med*. 2014;3:470-480.
32. Perng M-D, Wen S-F, Gibbon T, et al. Glial fibrillary acidic protein filaments can tolerate the incorporation of assembly-compromised GFAP-, but with consequences for filament organization and B-crystallin association. *Mol Biol Cell*. 2008;19:4521-4533.
33. De Filippis L, Lamorte G, Snyder EY, Malgaroli A, Vescovi AL. A novel, immortal, and multipotent human neural stem cell line generating functional neurons and oligodendrocytes. *Stem Cells*. 2007;25:2312-2321.
34. Kim M-S, Pinto SM, Getnet D, et al. A draft map of the human proteome. *Nature*. 2014;509:575-581.
35. Moeton M, Stassen OMJA, Sluijs JA, et al. GFAP isoforms control intermediate filament network dynamics, cell morphology, and focal adhesions. *Cell Mol Life Sci*. 2016;73:4101-4120.
36. Chen WJ, Liem RK. The endless story of the glial fibrillary acidic protein. *J. Cell Sci*. 1994;107(Pt 8):2299-2311.
37. Nielsen AL, Jorgensen AL. Self-assembly of the cytoskeletal glial fibrillary acidic protein is inhibited by an isoform-specific C terminus. *J Biol Chem*. 2004;279:41537-41545.
38. Jing R, Wilhelmsson U, Goodwill W, et al. Synemin is expressed in reactive astrocytes in neurotrauma and interacts differentially with vimentin and GFAP intermediate filament networks. *J Cell Sci*. 2007;120:1267-1277.
39. Jorgens DM, Inman JL, Wojcik M, et al. Deep nuclear invaginations are linked to cytoskeletal filaments - integrated bioimaging of epithelial cells in 3D culture. *J Cell Sci*. 2017;130:177-189.
40. Gudikote JP, Imam JS, Garcia RF, Wilkinson MF. RNA splicing promotes translation and RNA surveillance. *Nat Struct Amp Mol Biol*. 2005;12:801.
41. Chou Y-H, Flitney FW, Chang L, Mendez M, Grin B, Goldman RD. The motility and dynamic properties of intermediate filaments and their constituent proteins. *Exp Cell Res*. 2007;313:2236-2243.

SUPPORTING INFORMATION

Additional Supporting Information may be found online in the Supporting Information section.

How to cite this article: van Bodegraven EJ, Sluijs JA, Tan AK, Robe PAJT, Hol EM. New GFAP splice isoform (GFAPμ) differentially expressed in glioma translates into 21 kDa N-terminal GFAP protein. *The FASEB Journal*. 2021;35:e21389. https://doi.org/10.1096/fj.202001767R